



Intraretinal hyperreflective line: potential biomarker in various retinal disorders

Mustafa Kayabasi ¹, Seher Koksaldi ¹ and Ali Osman Saatci ²

¹ Department of Ophthalmology, Mus State Hospital, Mus, Turkey

² Department of Ophthalmology, Dokuz Eylul University, Izmir, Turkey

ABSTRACT

Background: The intraretinal hyperreflective line (IHL) is a novel posterior segment finding demonstrable using careful optical coherence tomography (OCT) examination. It likely indicates a reaction against photoreceptor, Muller cell, and/or retinal pigment epithelial damage. This study analyzed the spectral-domain OCT characteristics of IHLs to disclose their presence in various retinal conditions.

Methods: A retrospective review of the charted and imaging records of participants with IHL was conducted at Dokuz Eylul University Department of Ophthalmology between January 2019 and August 2023. The inclusion criterion was the detection of an IHL on good-quality B-scan spectral-domain OCT. An IHL was defined as a vertical line extending from the ellipsoid zone band (or lower) through the outer nuclear layer to the internal limiting membrane in the central fovea. Associated retinal conditions were recorded as potential causative factors for the presence of IHL.

Results: IHL was observed on spectral-domain OCT in 40 eyes of 38 participants with several retinal diseases assessment. Fourteen eyes (35%) underwent vitreoretinal surgery pre-IHL detection (12 were operated for full-thickness macular hole [FTMH], one for epiretinal membrane [ERM], and one for rhegmatogenous retinal detachment). In six eyes (15%) a microhole coexisted. Four eyes (10%) had a concurrent lamellar macular hole. The IHL preceded the occurrence of FTMH in three eyes (7.5%), and diabetic macular edema and type 2 idiopathic macular telangiectasia (MacTel-2) were present in three eyes (7.5%) each. The remaining conditions included vitreomacular traction (VMT), nonarteritic anterior ischemic optic neuropathy with central retinal artery occlusion, commotio retinae, exudative age-related macular degeneration, ERM, non-infectious idiopathic posterior uveitis, and Coats' disease, each affecting one eye (2.5%). Of the two participants with bilateral involvement, one was diagnosed with MacTel-2 and the other had IHL with VMT in the right eye that was detected post-vitreoretinal surgery for FTMH in the left eye.

Conclusions: Although IHLs are mostly identified in eyes with vitreomacular surface diseases, clinicians may encounter IHLs in other types of retinal pathology. Further large-scale, multicenter, long-term studies on the presence of IHLs in OCT imaging are required to provide more substantial insight on this biomarker.

KEYWORDS


retinal disease, intraretinal hyperreflective line, optical coherence tomography, vitreoretinal surgery, epiretinal membrane, macular holes, coats' disease, retinal telangiectases, nonarteritic anterior ischemic optic neuropathy, central retinal artery occlusion

Correspondence: Ali Osman Saatci, Department of Ophthalmology, Dokuz Eylul University, Izmir, Turkey. Email: osman.saatci@yahoo.com. ORCID iD: <https://orcid.org/0000-0001-6848-7239>

How to cite this article: Kayabasi M, Koksaldi S, Saatci AO. Intraretinal hyperreflective line: potential biomarker in various retinal disorders. *Med Hypothesis Discov Innov Ophthalmol*. 2024 Fall; 13(3): 129-138. <https://doi.org/10.51329/mehdiophthal1504>

Received: 23 July 2024; Accepted: 07 October 2024



Copyright © Author(s). This is an open-access article distributed under the terms of the Creative Commons Attribution-NonCommercial 4.0 International License (<https://creativecommons.org/licenses/by-nc/4.0/>) which permits copy and redistribute the material just in noncommercial usages, provided the original work is properly cited. 

INTRODUCTION

Intraretinal hyperreflective lines (IHLs) have been previously described using optical coherence tomography (OCT) in eyes with acquired vitelliform lesions [1-3], and may be a response to various types of damage faced by the photoreceptors, Muller cells, and/or retinal pigment epithelium (RPE) [1-3]. The Muller cell cone, a group of specialized central Muller cells that cover the foveolar floor, may serve a crucial function in enhancing the stability of the central foveola by mimicking glue [3]. Furthermore, IHLs signify the development of a full-thickness macular hole (FTMH), and appear to configure within the inner retina, originating at the base of the Muller cell cone [4].

IHLs have various names in the literature, including foveal crack sign [5, 6], cotton ball sign [7], hyperreflective central perpendicular line [8], hyperreflective stress line [3, 9], intraretinal hyperreflective foci [1], intraretinal hyperreflective line [2], and vertical hyperreflective track [4]. Although IHLs are mostly reported in association with FTMH and vitreomacular traction (VMT) [3, 5, 7], few studies have indicated a possible association with other retinal diseases [2, 10].

The primary objective in this single-center study was to demonstrate the presence of IHLs in distinct retinal conditions not previously documented.

METHODS

This retrospective observational case series was performed under the tenets of the Declaration of Helsinki and was approved by the local ethics committee of Dokuz Eylul University, Izmir, Turkey. In this study, routine spectral-domain OCT images obtained between January 2019 and September 2023 were retrospectively examined.

The sole inclusion criterion was the detection of an IHL on a good-quality (≥ 18 decibel [dB]) B-scan spectral-domain OCT. Associated retinal conditions were recorded as potential causative factors for the presence of IHL. Exclusion criteria were defined as the presence of any substantial coexisting media or lens opacity (cataract grade ≥ 3 according to the Emery–Little classification) [11] that could affect OCT image quality and OCT images of poor quality (signal-to-noise ratio < 18 dB) [12, 13].

A standardized comprehensive ophthalmic examination was conducted in all participants, including corrected distance visual acuity measurement using a Snellen chart (Auto Chart Projector CP 670; Nidek Co., Ltd., Gamagori, Japan), gonioscopy using a Goldmann three-mirror contact lens (Volk Optical Inc., OH, USA), anterior segment and dilated posterior segment examination under a slit lamp (Zeiss, Oberkochen, Germany), and intraocular pressure assessment (TonoRef II; Nidek Co.). OCT was performed using the Spectralis HRA + spectral-domain OCT device (Heidelberg Engineering, Heidelberg, Germany).

Clinical characteristics of the participants, including age, sex, and affected eye were obtained from the medical records per participant. For each eye demonstrating an IHL on a good-quality spectral-domain OCT scan, the following data were recorded: OCT image quality, central macular thickness (CMT), lens status, history of vitreoretinal surgery, and any associated retinal conditions. Two observers retrospectively reviewed the images for the presence of an IHL (M.K. and S.K.), and the senior author resolved any discrepancies (A.O.S.).

On spectral-domain OCT images, an IHL was defined as a vertical line extending from the ellipsoid zone band (or lower) through the outer nuclear layer to the internal limiting membrane (ILM) in the central fovea [1]. CMT was measured as the closest vertical distance from the RPE to the ILM, and an FTMH was defined as a full-thickness defect in the central fovea extending from the ILM to the RPE [14]. An epiretinal membrane (ERM) was defined as the presence of hyperreflective lines on the retina, parallel to the ILM, in conjunction with foveal pit deformation [14]. A lamellar macular hole (LMH) was defined as an irregular foveal configuration, thinning and disruption of the inner foveal region, absence of a complete foveal defect, and intact foveal photoreceptors [15]. The verifying of various retinal pathologies present in the participants was conducted according to relevant and widely accepted studies [14, 16-24].

Statistical analyses were conducted using IBM SPSS Statistics for Windows, version 26 (IBM Corp., Armonk, NY, USA). Normality of the data distribution was assessed using the Shapiro–Wilk test. Descriptive statistics are used to summarize the data, with categorical variables presented as counts and percentages, and quantitative variables reported as means (standard deviations [SD]).

RESULTS

From nearly 10 000 images acquired over a 5-year interval, 40 eyes of 38 participants were recruited according to the inclusion criteria. The detailed demographic and clinical characteristics of the study participants are presented in [Tables 1 and 2](#).

The right eyes of 20 participants, left eyes of 16 participants, and both eyes of two participants were included. The male-to-female ratio was 1:1, and the mean (SD) age of the entire cohort was 59.0 (17.0) years (range: 10–79 years). Among all eyes, 27 (67.5%) were phakic and 13 (32.5%) were pseudophakic. The mean (SD) OCT image quality and mean (SD) CMT for all eyes were 25.0 (4.6) dB (range: 18–36 dB) and 206.0 (63.4) μm (range: 132–498 μm), respectively (Tables 1 and 2).

Table 1. Demographic and clinical characteristics of the study participants

Variable	Value
Patients, n	38
Eyes, n	40
Age (y), Mean \pm SD	59.0 \pm 17.0
Sex (Male / Female), n (%)	19 (50) / 19 (50)
Unilateral / Bilateral, n (%)	36 (95) / 2 (5)
Laterality (OD / OS), n (%)	22 (55) / 18 (45)
Lens status (Phakic / Pseudophakic), n (%)	27 (67.5) / 13 (32.5)
The mean OCT image quality (dB), Mean \pm SD	25.0 \pm 4.6
The mean CMT (μm), Mean \pm SD	206.0 \pm 63.4

Abbreviations: n, numbers; y, years; SD, standard deviation; %, percentage; OD, right eye; OS, left eye; OCT, optical coherence tomography; dB, decibels; CMT, central macular thickness; μm , micrometers.

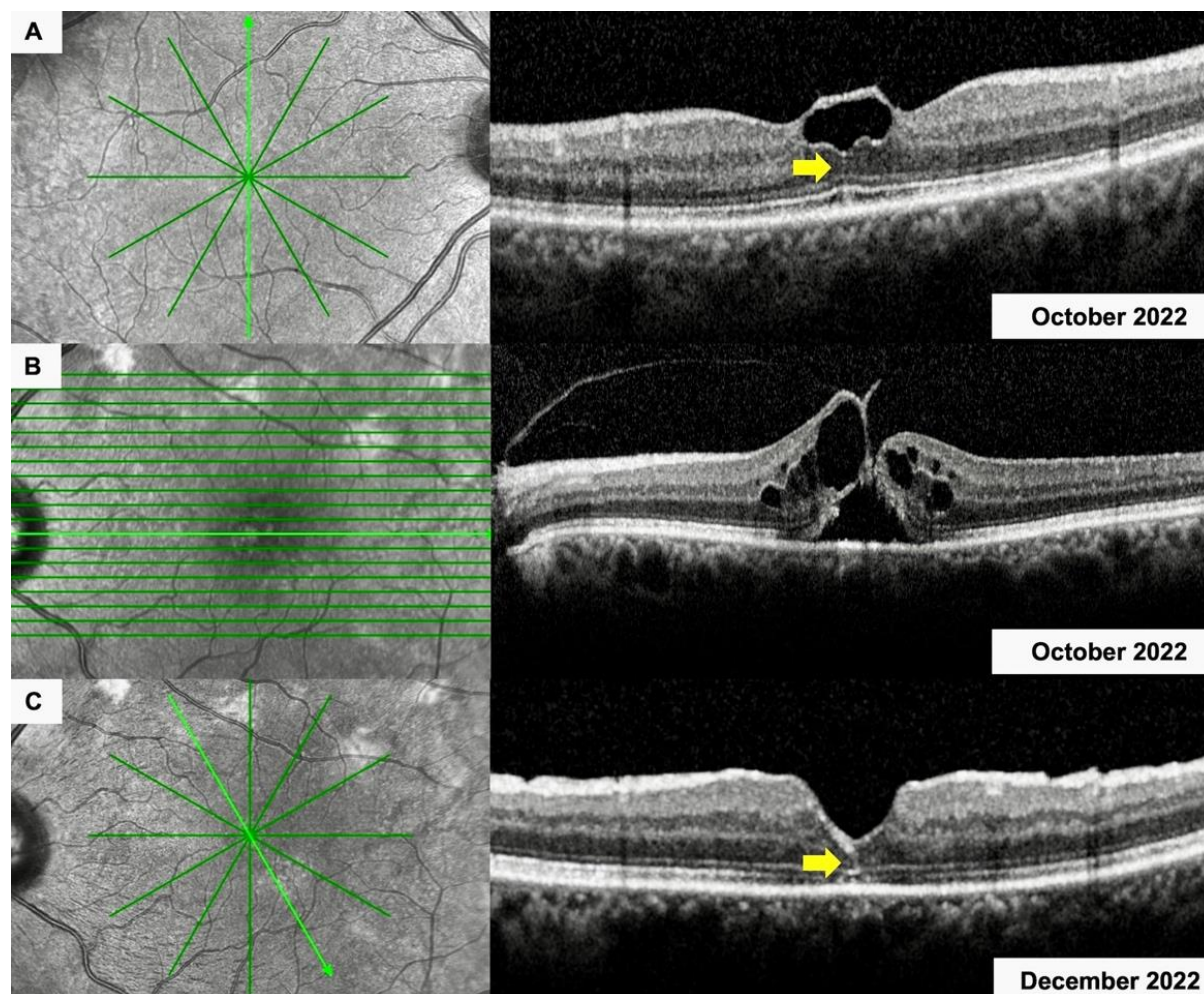


Figure 1. Spectral-domain optical coherence tomographic imaging of the right (A) and left (B, C) eye of a 63-year-old woman (Case 4) (Table 2) with (A) an intraretinal hyperreflective line (IHL) in her right eye (yellow arrow) and (B) vitreomacular traction and a full-thickness macular hole in her left eye. (C) Two months following vitreoretinal surgery, an IHL was detected in her left eye (yellow arrow), along with slightly disorganized foveal contour.

Table 2. Detailed demographic and clinical characteristics of study participants

Case No.	Age (y)	Sex	Laterality	Diagnosis	CMT (μm)	Lens status	Additional clinical information
1	69	M	OD	Diabetic macular edema.	213	Pseudophakic	Prior 32 intravitreal ranibizumab injections and 5 intravitreal dexamethasone implants.
2	71	M	OD	Lamellar macular hole.	167	Phakic	-
3	48	F	OS	After VRS for epiretinal membrane.	367	Phakic	Disorganization of inner retinal layers on OCT.
4	63	F	OD OS	Vitreomacular traction. After VRS for FTMH.	165 152	Phakic Phakic	-
5	61	M	OD	After VRS for FTMH.	244	Pseudophakic	Mild subfoveal fluid on OCT.
6	79	F	OS	Microhole.	214	Phakic	-
7	62	F	OD	After VRS for FTMH.	209	Pseudophakic	Steepening of the foveal contour.
8	61	M	OD OS	MacTel-2. MacTel-2.	198 194	Phakic Phakic	-
9	34	F	OD	NA-ION and central retinal artery occlusion.	498	Phakic	Second trimester of pregnancy.
10	13	M	OD	Microhole.	193	Phakic	-
11	10	F	OD	Microhole.	196	Phakic	-
12	66	F	OD	Exudative age-related macular degeneration.	200	Phakic	Prior 7 intravitreal aflibercept injections.
13	65	F	OS	After VRS for FTMH.	196	Phakic	-
14	72	M	OD	Lamellar macular hole.	183	Phakic	-
15	62	F	OS	After VRS for FTMH.	180	Pseudophakic	-
16	70	F	OS	Microhole.	162	Phakic	-
17	61	M	OS	Non-infectious idiopathic posterior uveitis.	225	Phakic	-
18	59	F	OD	MacTel-2.	224	Phakic	-
19	77	F	OD	Microhole.	191	Pseudophakic	-
20	68	F	OD	Lamellar macular hole.	232	Phakic	-
21	74	F	OS	Epiretinal membrane.	270	Phakic	-
22	61	M	OS	After VRS for FTMH.	176	Pseudophakic	Loss of the subfoveal ellipsoid zone on OCT.
23	64	F	OD	After VRS for FTMH.	138	Pseudophakic	Steepening of the foveal contour.
24	67	F	OD	Microhole.	191	Phakic	-
25	53	M	OS	After VRS for rhegmatogenous retinal detachment.	132	Phakic	Disorganization of the ellipsoid zone on OCT.
26	10	M	OS	Coats' disease.	172	Phakic	Prior 2 intravitreal dexamethasone implants.
27	51	M	OD	Lamellar macular hole.	239	Phakic	-
28	66	M	OS	Before FTMH.	155	Phakic	-
29	74	F	OD	After VRS for FTMH.	184	Pseudophakic	-
30	65	M	OD	Before FTMH.	161	Phakic	-
31	65	M	OS	Diabetic macular edema.	215	Phakic	Prior 2 intravitreal ranibizumab injections.
32	74	M	OS	After VRS for FTMH.	251	Pseudophakic	-
33	70	M	OD	Before FTMH.	187	Pseudophakic	-
34	64	F	OD	After VRS for FTMH.	160	Pseudophakic	-
35	61	F	OD	After VRS for FTMH.	170	Pseudophakic	-
36	40	M	OS	Comotio retinae.	192	Phakic	-
37	60	M	OS	Diabetic macular edema.	264	Phakic	Prior 31 intravitreal aflibercept injection and 2 intravitreal dexamethasone implants.
38	50	M	OS	After VRS for FTMH,	181	Pseudophakic	-

Abbreviations: y, years; CMT, central macular thickness; μm , micrometers; M, male; OD, right eye; F, female; OS, left eye; VRS, vitreoretinal surgery; OCT, optical coherence tomography; FTMH, full-thickness macular hole; MacTel-2, type-2 idiopathic macular telangiectasia; NA-ION, non-arteritic anterior ischemic optic neuropathy.

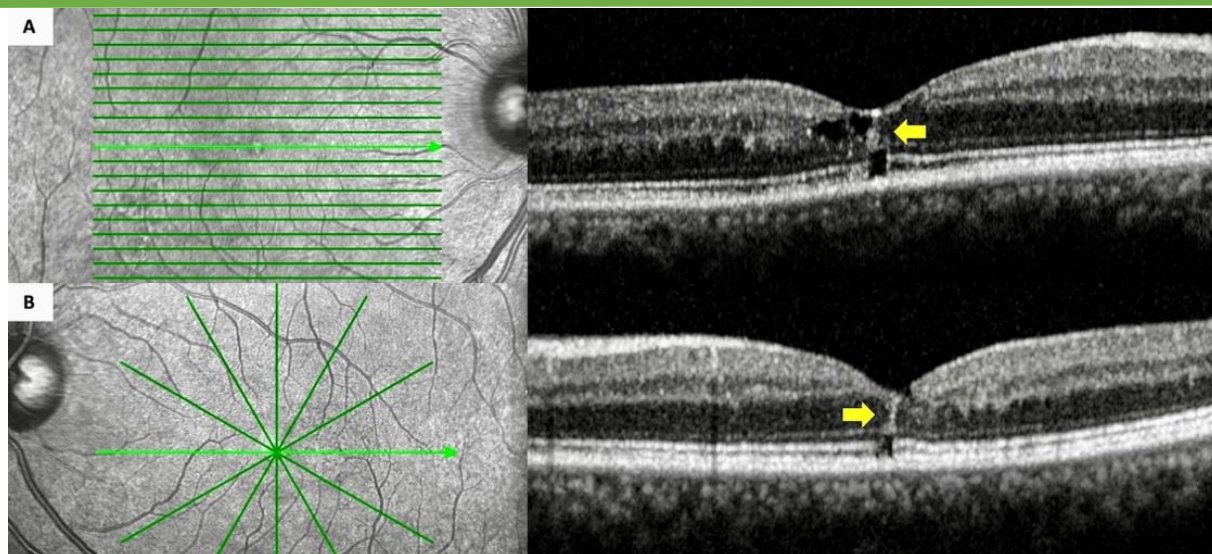


Figure 2. Spectral-domain optical coherence tomographic imaging of the right (A) and left (B) eye of a 61-year-old man (Case 8) (Table 2) with type 2 idiopathic macular telangiectasia (A and B) featuring bilateral intraretinal hyperreflective lines (yellow arrows) on transfoveal sections. (A and B) Bilateral microhole formation was also present.

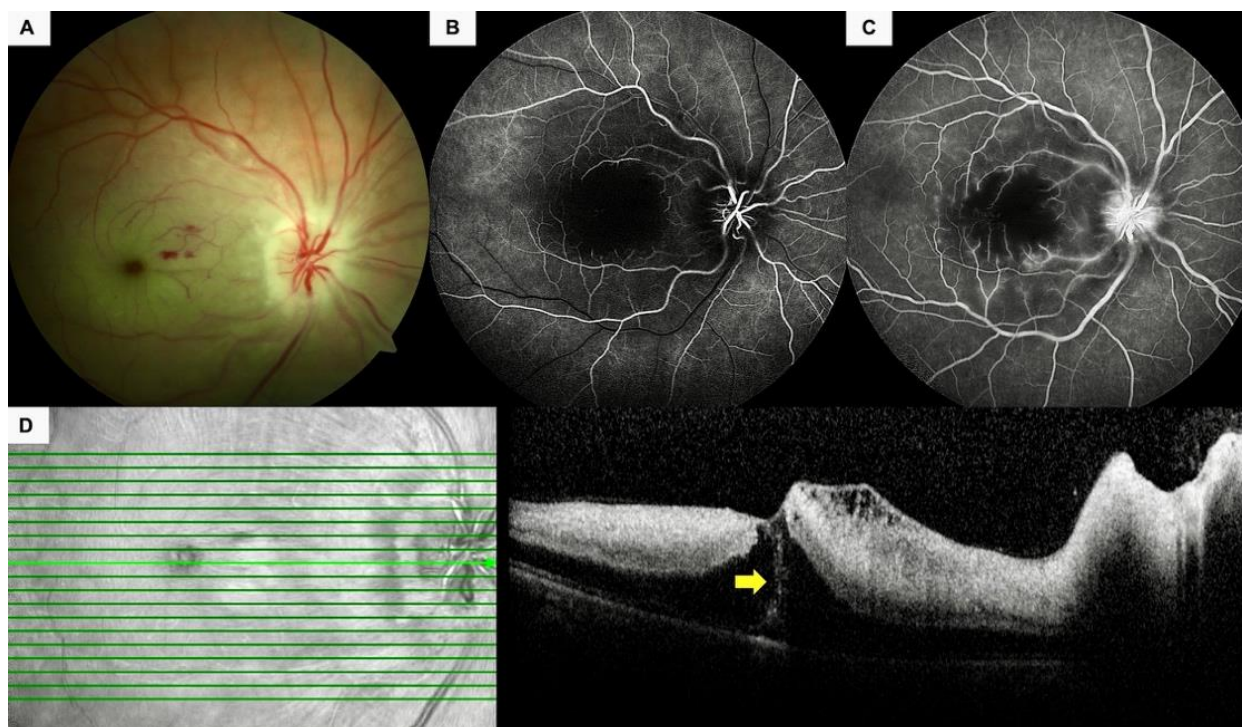


Figure 3. A 34-year-old pregnant woman (Case 9) (Table 2) presented with painless, sudden-onset vision loss in her right eye. (A) Color fundus photographs depicted an infarcted macula, pale and swollen optic nerve head, and a few intraretinal hemorrhages. (B) The early phase of a fluorescein angiogram revealed the nonperfused foveola and late filling of the arterioles. (C) Some pinpoint leakages from the macular retinal arterioles and faint optic disc leakage was noted in the late-phase fluorescein angiogram. (D) Spectral-domain optical coherence tomography revealed retinal thickening, increased hyperreflectivity of the inner retinal layers, and an intraretinal hyperreflective line (yellow arrow).

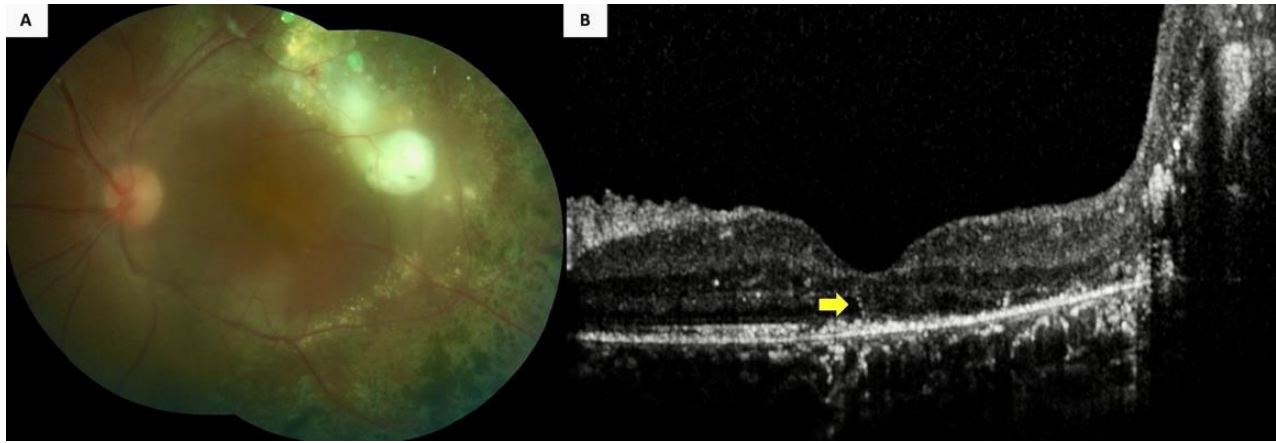


Figure 4. A 10-year-old boy (Case 26) (Table 2) with Coats’ disease displayed (A) extensive retinal exudation and photocoagulation scars in his left eye, along with a serous retinal detachment at the temporal macular aspect. Furthermore, the color fundus photograph was blurred because of a posterior subcapsular cataract. However, (B) an intraretinal hyperreflective line was visible (yellow arrow) on the spectral-domain optical coherence tomographic section passing through the fovea, along with a massive exudation at the temporal aspect.

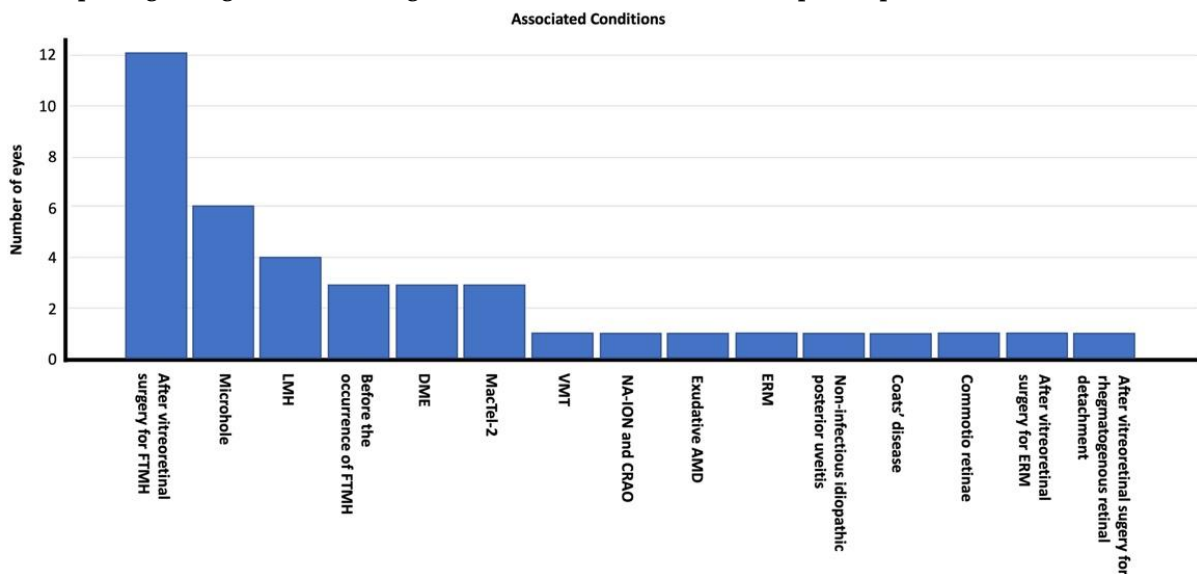


Figure 5. Distribution of the associated retinal diseases among the study participants.

Abbreviations: FTMH, full-thickness macular hole; LMH, lamellar macular hole; DME, diabetic macular edema; MacTel-2, type-2 idiopathic macular telangiectasia; VMT, vitreomacular traction; NA-ION, non-arteritic anterior ischemic optic neuropathy; CRAO, central retinal artery occlusion; AMD, age-related macular degeneration, ERM; epiretinal membrane.

Of the 40 eyes exhibiting an IHL on spectral-domain OCT sections, various associated conditions were identified. Fourteen eyes (35%) had undergone vitreoretinal surgery pre-IHL detection (12 had surgery for FTMH, one for ERM, and one for rhegmatogenous retinal detachment; Figure 1). In six eyes (15%), the IHL was accompanied by microhole formation, and four eyes (10%) had concurrent LMH. The IHL preceded the occurrence of an FTMH in three eyes (7.5%), and diabetic macular edema (DME) and type 2 idiopathic macular telangiectasia (MacTel-2; Figure 2) were present in three eyes (7.5%) each. The remaining conditions included VMT, non-arteritic anterior ischemic optic neuropathy (NA-ION) with central retinal artery occlusion (CRAO; Figure 3), commotio retinae, exudative age-related macular degeneration (AMD), ERM, non-infectious idiopathic posterior uveitis, and Coats’ disease (Figure 4), each affecting one eye each (2.5%). Figure 5 displays the distribution of the associated conditions among the studied eyes.

Of the two participants with bilateral involvement, one (Case 8) (Table 2) was diagnosed with MacTel-2 (Figure 2), and the other with IHL associated with VMT in the right eye (Case 4; Table 2), and was detected 2 months after vitreoretinal surgery for FTMH in the left eye (Figure 1).

Vitreoretinal surgery had been performed in 14 eyes (35%) pre-IHL detection on spectral-domain OCT, and five eyes (12.5%) had prior intravitreal injections. One eye (2.5%) had received 32 prior intravitreal ranibizumab injections (Lucentis; Novartis Pharma AG, Basel, Switzerland) and five prior intravitreal dexamethasone (Ozurdex, Allergan, Dublin, Ireland) implants for DME; one eye (2.5%) had been treated with 31 intravitreal aflibercept injections (Eylea, Bayer, Leverkusen, Germany) and two intravitreal dexamethasone implants for DME; one eye (2.5%) had received seven intravitreal aflibercept injections for exudative AMD; one eye (2.5%) had undergone two intravitreal ranibizumab injections for DME; and the remaining eye (2.5%) had received two intravitreal dexamethasone implants for Coats' disease (Table 2) pre-IHL identification.

DISCUSSION

In the present study, IHLs most frequently occurred following vitreoretinal surgery, particularly for FTMH. To the best of our knowledge, this is the first report of the presence of IHLs in several other retinal diseases, such as DME, MacTel-2, NA-ION with CRAO, commotio retinae, non-infectious idiopathic posterior uveitis, and Coats' disease.

Scharf et al. [3] retrospectively examined 181 eyes (93 eyes with FTMH and 88 eyes with LMH) and identified a vertical hyperreflective line preceding FTMH development in six of 12 eyes (50%) with available spectral-domain OCT scans acquired prior to the occurrence of FTMH. In contrast, 22 of 88 eyes (25%) with LMH exhibited a concurrent vertical hyperreflective line on spectral-domain OCT images. Briefly, Scharf et al. [3] concluded that the vertical hyperreflective line potentially originated from a central foveal dehiscence associated with the disruption of the Muller cell cone. Thus, a vertical hyperreflective line on OCT examination could serve as an early clinical indicator of VMT and impending development of MH [3]. Furthermore, the findings of this study support their results, as the IHLs were associated with LMH in four eyes (10%) and were observed prior to FTMH discovery in three eyes (7.5%) and VMT in one eye (2.5%).

MacTel-2 is a retinal pathology that predominantly affects the macular Muller cells [25]. Therefore, Muller cell cone damage may be the main mechanism underlying the IHL observed in patients with MacTel-2.

Guixeres Esteve and Postelmans [8] examined the spectral-domain OCT findings of a hyperreflective perpendicular central line in five eyes of four patients with no history of MH or unexplained loss of visual acuity; however, all exhibited vitreofoveal adhesion [8]. They proposed that a hyperreflective perpendicular central line was a sign of VMT, and observed that a single eye developed FTMH several weeks after phacoemulsification surgery [8]. In our study, 13 eyes (32.5%) had undergone uneventful cataract surgery pre-IHL detection.

Using OCT images, Ishibashi et al. [5] evaluated 10 eyes of 10 patients who experienced secondary MH formation following pars plana vitrectomy performed for rhegmatogenous retinal detachment. They demonstrated that all eyes had a parafoveal ERM and foveal crack sign, a characteristic OCT finding (i.e., a hyperreflective vertical line in the foveola with foveal deformation) pre-MH formation. Therefore, they hypothesized that the presence of the foveal crack predicts secondary MH formation due to ERM traction [5]. Meanwhile, in this study, we observed IHLs in 14 eyes (35%) following vitreoretinal surgery: 12 were for FTMH, one for ERM, and one for rhegmatogenous retinal detachment, confirming vitreoretinal surgery as the most commonly associated factor for IHL occurrence. Additionally, an IHL in one eye (Case 21) with ERM but without any prior vitreoretinal surgery was observed, suggesting that ERM traction may be a possible inciting factor for IHL formation.

Furashova and Matthe [6] evaluated 113 fellow eyes of 113 patients with FTMH using spectral-domain OCT images to investigate the prevalence and predictive value of the foveal crack sign. They delineated a foveal crack sign in 19 of 113 fellow eyes (17%), and 10 progressed to FTMH during a mean follow-up period of 21 months. Two other eyes with FTMH formation had no foveal crack sign at baseline. Progression was reported in 10 of 13 eyes (77%) in patients with foveal crack sign and vitreous adhesion, none in the six eyes of patients with foveal crack sign and vitreous detachment, two of 48 eyes (4%) in patients with vitreous adhesion but without the foveal crack sign, and none in the 46 eyes of patients with vitreous detachment and without the foveal crack sign [6]. The sensitivity and specificity of the foveal crack sign in predicting FTMH formation were determined as 83.3 and 91.1%, respectively. The positive and negative predictive values of the foveal crack sign were estimated as 52.6 and 97.9%, respectively. The authors concluded that fellow eyes with the foveal crack sign in patients with FTMH are at very high risk (77%) of FTMH development if posterior vitreous adhesion is present [6]. Herein, the IHL preceded the occurrence of FTMH in three eyes (7.5%); IHL was associated with VMT in the right eye of one participant, whereas it was detected 2 months post-vitreoretinal surgery for FTMH in the left eye.

Amoroso et al. [2] retrospectively reviewed the color fundus photographs, autofluorescence, spectral-domain OCT, and fluorescein and/or indocyanine green angiography images of 49 eyes of 43 patients (16 men and 27 women). IHLs were classified as linear or curvilinear by their orientation on OCT sections, and as thick or thin depending on their thickness. They found that linear hyperreflective vertical lines (38 eyes) or curvilinear lines along the Henle fiber layer (HFL; 11 eyes) were present in association with various macular conditions, as follows: adult vitelliform dystrophy or pattern dystrophy (24 eyes), ERM (six eyes), thick choroid (nine eyes), AMD (nine eyes), partial resorption of subretinal or intraretinal hemorrhages (five eyes), idiopathic macular microhole (two eyes), VMT (three eyes), multiple evanescent white dot syndrome (MEWDS; three eyes), fundus flavimaculatus (two eyes), and pachychoroid pigment epitheliopathy (one eye) [2]. They also reported that hemorrhagic or inflammatory IHLs were transient and showed full regression in their cohort. IHLs observed in association with VMT usually regressed slowly during follow-up. In contrast, IHLs associated with acquired vitelliform lesions or AMD persisted without significant changes in most cases, except when geographic atrophy or exudative AMD occurred [2]. In addition, in MEWDS cases, inflammatory damage to the central cones and Muller cells induces IHLs, whereas in VMT cases, structural destabilization of the central cones and Muller cells were secondary factors of IHLs occurrence [2]. Thus, inflammatory damage and structural destabilization of the retinal layers are potential causative factors for IHL, and the presence of IHLs in cases with vascular diseases such as DME, NA-ION with CRAO, MacTel-2, and Coats' disease, possibly suggest an underlying vascular involvement in IHL formation.

Acute retinal pigment epitheliitis (ARPE) is a retinal condition that is associated with IHLs [10, 26]. Cho et al. [26] reported the presence of an abnormal hyperreflectivity extending from the inner RPE layer to the outer nuclear layer in an ARPE case. The IHL resolved along with the disruption of the ellipsoid zone, in this patient [26]. Singh et al. [10] described a 39-year-old female patient with IHLs and ARPE. They hypothesized the composition of the IHLs were RPE cells, blood components, or inflammatory cells, all exhibiting a hyperreflectivity on OCT images that is similar to that of subretinal hyperreflective exudative material [10]. None of our participants had a diagnosis of ARPE.

Ramtohul et al. [27] introduced the novel OCT terminology "angular sign of HFL hyperreflectivity" to indicate the disruption of the entire photoreceptor length, including the HFL, in various macular diseases such as acute macular neuroretinopathy, Dengue maculopathy, whiplash maculopathy, contusion maculopathy, paracentral acute middle maculopathy, and ARPE [27]. Furthermore, they designated another OCT finding characterized by a vertical, linear, hyperreflective lesion at the central fovea as the "hyperreflective stress line," emphasizing the importance of distinguishing between these two OCT findings due to their distinct underlying pathophysiological mechanisms [27]. However, Amoroso et al. [2] categorized these two findings as different manifestations within the same spectrum [2]. Additionally, in this study, the observed IHLs were more likely to correspond with the linear hyperreflective vertical lines described by Amoroso et al. [2]. As the linear and curvilinear hyperreflective lines might have represented distinct pathophysiological cellular processes, we did not consider these two findings to be within the same spectrum and did not categorize the IHLs in our participants as linear or curvilinear.

In the current technological era, artificial intelligence is widely used for the diagnosis and screening of various ophthalmological conditions, including retinal disorders [28-30]. Waldstein et al. [31] investigated the characterization of hyperreflective foci in patients with AMD using artificial intelligence algorithms and spatiotemporal atlas methods. They analyzed 8529 OCT sections of 512 patients and reported that the eyes progressing to advanced AMD had higher hyperreflective foci volume and an accelerated increase in hyperreflective foci activity. Thus, the development of an atlas of retinal changes in the aging eye using artificial intelligence would improve the comprehension of the pathological features of AMD [31]. Similar studies on the detection and screening of IHLs using artificial intelligence could be conducted in the future to show the clinical importance of these lesions in various diseases.

The present study supports the findings of previous research by demonstrating IHLs in a substantial number of patients and in eyes with varying diagnoses, yet it features several limitations, mostly related to its retrospective nature. As the choroidal thickness and curvilinear lines along the HFL were not evaluated, and follow-up examinations could not be performed in most cases; therefore, we could not observe how IHL evolved over time. The prevalence and predictive value of IHLs were not determined; thus, the prognostic importance of IHLs remained unclear. Further prospective studies with longitudinal follow-ups are required to assess the implications and clinical value of IHLs as a novel OCT sign in various retinal disorders. Despite its limitations, this is the first study to report on the occurrence of IHLs in specific conditions such as DME, MacTel-2, NA-ION with CRAO, commotio retinae, non-infectious idiopathic posterior uveitis, and Coats' disease.

CONCLUSIONS

Different terminology exists in the literature on the description and significance of IHL formation, and this particular OCT finding has been primarily reported as either a preceding indicator for FTMH development or as a coexisting finding alongside VMT. However, our study concludes that IHLs might occur in diverse retinal conditions including vascular or inflammatory processes. Therefore, recognizing this sign may aid clinicians to predict prognosis during patient follow-up. Future large-scale, long-term, multicenter studies on the presence of IHLs in OCT imaging are required to foster genuine insight into this biomarker.

ETHICAL DECLARATIONS

Ethical approval: This retrospective observational case series was performed under the tenets of the Declaration of Helsinki and was approved by the local ethics committee of Dokuz Eylul University, Izmir, Turkey.

Conflict of interest: None.

FUNDING

None.

ACKNOWLEDGMENTS

None.

REFERENCES

- Chen KC, Jung JJ, Curcio CA, Balaratnasingam C, Gallego-Pinazo R, Dolz-Marco R, Freund KB, Yannuzzi LA. Intraretinal Hyperreflective Foci in Acquired Vitelliform Lesions of the Macula: Clinical and Histologic Study. *Am J Ophthalmol*. 2016 Apr;164:89-98. doi: 10.1016/j.ajo.2016.02.002. Epub 2016 Feb 8. PMID: 26868959.
- Amoroso F, Mrejen S, Pedinielli A, Tabary S, Souied EH, Gaudric A, Cohen SY. INTRARETINAL HYPERREFLECTIVE LINES. *Retina*. 2021 Jan 1;41(1):82-92. doi: 10.1097/IAE.0000000000002806. PMID: 32251237.
- Scharf JM, Hilely A, Preti RC, Grondin C, Chehaibou I, Greaves G, Tran K, Wang D, Ip MS, Hubschman JP, Gaudric A, Sarraf D. Hyperreflective Stress Lines and Macular Holes. *Invest Ophthalmol Vis Sci*. 2020 Apr 9;61(4):50. doi: 10.1167/iovs.61.4.50. PMID: 32347919; PMCID: PMC7401923.
- Padhy SK, Tripathy K. Commentary: Clinical significance of vertical hyper-reflective track in optical coherence tomography of the fovea. *Indian Journal of Ophthalmology-Case Reports*. 2022 Apr 1;2(2):473-4. doi: 10.4103/ijo.IJO_62_22.
- Ishibashi T, Iwama Y, Nakashima H, Ikeda T, Emi K. Foveal Crack Sign: An OCT Sign Preceding Macular Hole After Vitrectomy for Rhegmatogenous Retinal Detachment. *Am J Ophthalmol*. 2020 Oct;218:192-198. doi: 10.1016/j.ajo.2020.05.030. Epub 2020 May 29. PMID: 32479809.
- Furashova O, Matthé E. Foveal crack sign as a predictive biomarker for development of macular hole in fellow eyes of patients with full-thickness macular holes. *Sci Rep*. 2020 Nov 16;10(1):19932. doi: 10.1038/s41598-020-77078-y. PMID: 33199791; PMCID: PMC7670431.
- Tsunoda K, Watanabe K, Akiyama K, Usui T, Noda T. Highly reflective foveal region in optical coherence tomography in eyes with vitreomacular traction or epiretinal membrane. *Ophthalmology*. 2012 Mar;119(3):581-7. doi: 10.1016/j.ophtha.2011.08.026. Epub 2011 Nov 23. PMID: 22115711.
- Guixeres Esteve MC, Postelmans L. Central perpendicular line in macular spectral-domain optical coherence tomography in five eyes. *Eur J Ophthalmol*. 2020 Mar;30(2):NP16-NP22. doi: 10.1177/1120672119834476. Epub 2019 Mar 14. PMID: 30866678.
- Preti RC, Zacharias LC, Cunha LP, Monteiro MLR, Sarraf D. Spontaneous macular hole closure after posterior vitreous detachment in an eye with hyperreflective OCT stress line. *Am J Ophthalmol Case Rep*. 2020 Sep 29;20:100950. doi: 10.1016/j.ajoc.2020.100950. PMID: 33195877; PMCID: PMC7644851.
- Singh A, Beg H, Gaur R, Kothari A, Chugh M, Gorhe S, Saurabh K, Roy R. Intraretinal hyperreflective line in association with acute retinal pigment epithelitis. *Indian Journal of Ophthalmology-Case Reports*. 2022 Jul 1;2(3):691-3. doi: 10.4103/ijo.IJO_2020_21.
- Xu K, Hao Y. Determination of the density of human nuclear cataract lenses. *Mol Med Rep*. 2013 Nov;8(5):1300-4. doi: 10.3892/mmr.2013.1673. Epub 2013 Sep 9. PMID: 24026512; PMCID: PMC3820609.
- Liu S, Paranjape AS, Elmaanaoui B, Dewelle J, Rylander HG 3rd, Markey MK, Milner TE. Quality assessment for spectral domain optical coherence tomography (OCT) images. *Proc SPIE Int Soc Opt Eng*. 2009;7171:71710X. doi: 10.1117/12.809404. PMID: 20431701; PMCID: PMC2860632.
- Zicarelli F, Ometto G, Montesano G, Motta S, De Simone L, Cimino L, Staurenghi G, Agarwal A, Pichi F, Invernizzi A. Objective Quantification of Posterior Segment Inflammation: Measuring Vitreous Cells and Haze Using Optical

- Coherence Tomography. *Am J Ophthalmol.* 2023 Jan;245:134-144. doi: [10.1016/j.ajo.2022.08.025](https://doi.org/10.1016/j.ajo.2022.08.025). Epub 2022 Sep 7. PMID: [36084686](https://pubmed.ncbi.nlm.nih.gov/36084686/).
14. Duker JS, Kaiser PK, Binder S, de Smet MD, Gaudric A, Reichel E, Sadda SR, Sebag J, Spaide RF, Stalmans P. The International Vitreomacular Traction Study Group classification of vitreomacular adhesion, traction, and macular hole. *Ophthalmology.* 2013 Dec;120(12):2611-2619. doi: [10.1016/j.ophtha.2013.07.042](https://doi.org/10.1016/j.ophtha.2013.07.042). Epub 2013 Sep 17. PMID: [24053995](https://pubmed.ncbi.nlm.nih.gov/24053995/).
 15. Frisina R, Pilotto E, Midena E. Lamellar Macular Hole: State of the Art. *Ophthalmic Res.* 2019;61(2):73-82. doi: [10.1159/000494687](https://doi.org/10.1159/000494687). Epub 2019 Jan 9. PMID: [30625477](https://pubmed.ncbi.nlm.nih.gov/30625477/).
 16. Strøm C, Sander B, Larsen N, Larsen M, Lund-Andersen H. Diabetic macular edema assessed with optical coherence tomography and stereo fundus photography. *Invest Ophthalmol Vis Sci.* 2002 Jan;43(1):241-5. PMID: [11773037](https://pubmed.ncbi.nlm.nih.gov/11773037/).
 17. Paunescu LA, Ko TH, Duker JS, Chan A, Drexler W, Schuman JS, Fujimoto JG. Idiopathic juxtafoveal retinal telangiectasis: new findings by ultrahigh-resolution optical coherence tomography. *Ophthalmology.* 2006 Jan;113(1):48-57. doi: [10.1016/j.ophtha.2005.08.016](https://doi.org/10.1016/j.ophtha.2005.08.016). Epub 2005 Dec 15. PMID: [16343625](https://pubmed.ncbi.nlm.nih.gov/16343625/); PMCID: [PMC1941653](https://pubmed.ncbi.nlm.nih.gov/PMC1941653/).
 18. Patil AD, Bioussé V, Newman NJ. Ischemic Optic Neuropathies: Current Concepts. *Ann Indian Acad Neurol.* 2022 Oct;25(Suppl 2):S54-S58. doi: [10.4103/aian.aian_533_22](https://doi.org/10.4103/aian.aian_533_22). Epub 2022 Aug 8. PMID: [36589029](https://pubmed.ncbi.nlm.nih.gov/36589029/); PMCID: [PMC9795705](https://pubmed.ncbi.nlm.nih.gov/PMC9795705/).
 19. Ahn SJ, Woo SJ, Park KH, Jung C, Hong JH, Han MK. Retinal and choroidal changes and visual outcome in central retinal artery occlusion: an optical coherence tomography study. *Am J Ophthalmol.* 2015 Apr;159(4):667-76. doi: [10.1016/j.ajo.2015.01.001](https://doi.org/10.1016/j.ajo.2015.01.001). Epub 2015 Jan 9. PMID: [25579642](https://pubmed.ncbi.nlm.nih.gov/25579642/).
 20. Hubschman JP, Govetto A, Spaide RF, Schumann R, Steel D, Figueroa MS, Sebag J, Gaudric A, Staurengi G, Haritoglou C, Kadosono K, Thompson JT, Chang S, Bottoni F, Tadayoni R. Optical coherence tomography-based consensus definition for lamellar macular hole. *Br J Ophthalmol.* 2020 Dec;104(12):1741-1747. doi: [10.1136/bjophthalmol-2019-315432](https://doi.org/10.1136/bjophthalmol-2019-315432). Epub 2020 Feb 27. PMID: [32107208](https://pubmed.ncbi.nlm.nih.gov/32107208/).
 21. Velaga SB, Nittala MG, Konduru RK, Heussen F, Keane PA, Sadda SR. Impact of optical coherence tomography scanning density on quantitative analyses in neovascular age-related macular degeneration. *Eye (Lond).* 2017 Jan;31(1):53-61. doi: [10.1038/eye.2016.260](https://doi.org/10.1038/eye.2016.260). Epub 2016 Dec 2. PMID: [27911444](https://pubmed.ncbi.nlm.nih.gov/27911444/); PMCID: [PMC5233945](https://pubmed.ncbi.nlm.nih.gov/PMC5233945/).
 22. Jabs DA, Nussenblatt RB, Rosenbaum JT; Standardization of Uveitis Nomenclature (SUN) Working Group. Standardization of uveitis nomenclature for reporting clinical data. Results of the First International Workshop. *Am J Ophthalmol.* 2005 Sep;140(3):509-16. doi: [10.1016/j.ajo.2005.03.057](https://doi.org/10.1016/j.ajo.2005.03.057). PMID: [16196117](https://pubmed.ncbi.nlm.nih.gov/16196117/); PMCID: [PMC8935739](https://pubmed.ncbi.nlm.nih.gov/PMC8935739/).
 23. Sony P, Venkatesh P, Gadaginamath S, Garg SP. Optical coherence tomography findings in commotio retina. *Clin Exp Ophthalmol.* 2006 Aug;34(6):621-3. doi: [10.1111/j.1442-9071.2006.01290.x](https://doi.org/10.1111/j.1442-9071.2006.01290.x). PMID: [16925718](https://pubmed.ncbi.nlm.nih.gov/16925718/).
 24. Yasuno Y, Miura M, Kawana K, Makita S, Sato M, Okamoto F, Yamanari M, Iwasaki T, Yatagai T, Oshika T. Visualization of sub-retinal pigment epithelium morphologies of exudative macular diseases by high-penetration optical coherence tomography. *Invest Ophthalmol Vis Sci.* 2009 Jan;50(1):405-13. doi: [10.1167/iovs.08-2272](https://doi.org/10.1167/iovs.08-2272). Epub 2008 Aug 1. PMID: [18676629](https://pubmed.ncbi.nlm.nih.gov/18676629/).
 25. Kedariseti KC, Narayanan R, Stewart MW, Reddy Gurram N, Khanani AM. Macular Telangiectasia Type 2: A Comprehensive Review. *Clin Ophthalmol.* 2022 Oct 10;16:3297-3309. doi: [10.2147/OPTH.S373538](https://doi.org/10.2147/OPTH.S373538). PMID: [36237488](https://pubmed.ncbi.nlm.nih.gov/36237488/); PMCID: [PMC9553319](https://pubmed.ncbi.nlm.nih.gov/PMC9553319/).
 26. Cho HJ, Han SY, Cho SW, Lee DW, Lee TG, Kim CG, Kim JW. Acute retinal pigment epitheliitis: spectral-domain optical coherence tomography findings in 18 cases. *Invest Ophthalmol Vis Sci.* 2014 May 1;55(5):3314-9. doi: [10.1167/iovs.14-14324](https://doi.org/10.1167/iovs.14-14324). PMID: [24787563](https://pubmed.ncbi.nlm.nih.gov/24787563/).
 27. Ramtohul P, Cabral D, Sadda S, Freund KB, Sarraf D. The OCT angular sign of Henle fiber layer (HFL) hyperreflectivity (ASHH) and the pathoanatomy of the HFL in macular disease. *Prog Retin Eye Res.* 2023 Jul;95:101135. doi: [10.1016/j.preteyeres.2022.101135](https://doi.org/10.1016/j.preteyeres.2022.101135). Epub 2022 Nov 1. PMID: [36333227](https://pubmed.ncbi.nlm.nih.gov/36333227/).
 28. Oganov AC, Seddon I, Jabbehdari S, Uner OE, Fonoudi H, Yazdanpanah G, Outani O, Arevalo JF. Artificial intelligence in retinal image analysis: Development, advances, and challenges. *Surv Ophthalmol.* 2023 Sep-Oct;68(5):905-919. doi: [10.1016/j.survophthal.2023.04.001](https://doi.org/10.1016/j.survophthal.2023.04.001). Epub 2023 Apr 26. PMID: [37116544](https://pubmed.ncbi.nlm.nih.gov/37116544/).
 29. Hormel TT, Hwang TS, Bailey ST, Wilson DJ, Huang D, Jia Y. Artificial intelligence in OCT angiography. *Prog Retin Eye Res.* 2021 Nov;85:100965. doi: [10.1016/j.preteyeres.2021.100965](https://doi.org/10.1016/j.preteyeres.2021.100965). Epub 2021 Mar 22. PMID: [33766775](https://pubmed.ncbi.nlm.nih.gov/33766775/); PMCID: [PMC8455727](https://pubmed.ncbi.nlm.nih.gov/PMC8455727/).
 30. Maceroni M, Monforte M, Cariola R, Falsini B, Rizzo S, Savastano MC, Martelli F, Ricci E, Bortolani S, Tasca G, Minnella AM. Artificial Intelligence for Evaluation of Retinal Vasculopathy in Facioscapulohumeral Dystrophy Using OCT Angiography: A Case Series. *Diagnostics (Basel).* 2023 Mar 4;13(5):982. doi: [10.3390/diagnostics13050982](https://doi.org/10.3390/diagnostics13050982). PMID: [36900126](https://pubmed.ncbi.nlm.nih.gov/36900126/); PMCID: [PMC10001401](https://pubmed.ncbi.nlm.nih.gov/PMC10001401/).
 31. Waldstein SM, Vogl WD, Bogunovic H, Sadeghipour A, Riedl S, Schmidt-Erfurth U. Characterization of Drusen and Hyperreflective Foci as Biomarkers for Disease Progression in Age-Related Macular Degeneration Using Artificial Intelligence in Optical Coherence Tomography. *JAMA Ophthalmol.* 2020 Jul 1;138(7):740-747. doi: [10.1001/jamaophthalmol.2020.1376](https://doi.org/10.1001/jamaophthalmol.2020.1376). PMID: [32379287](https://pubmed.ncbi.nlm.nih.gov/32379287/); PMCID: [PMC7206537](https://pubmed.ncbi.nlm.nih.gov/PMC7206537/).